
Automated contour segmentation for treatment planning: challenges and potentials

Minsong Cao, Ph.D.

Department of Radiation Oncology
University of California, Los Angeles
UCLA



Learning objectives

- To review the current state-of-the-art methods on automated contour segmentation for treatment planning
- To understand the challenges and potentials on automated contour segmentation



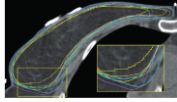
Disclosure

- None



Background

- Clinical contouring is critical for treatment planning:
 - directly impact dosimetry quality and clinical decision
 - time consuming and labor intensive
- Contour is one of the largest sources of dosimetric uncertainty
 - contour error and variation
 - quality of contouring:
 - spatial accuracy
 - dosimetric accuracy



Jameson M. et al. J Medl Img Radit Onc 54 (2010)



UCLA Health

Automated contour segmentation

- Seek to reduce time and inter-observer variability
- Clinical applications:
 - Standard treatment planning
 - Adaptive treatment planning
 - Motion tracking and gating
- Commercial products available, but not frequently used in clinical practice
- Conflict findings reported on contour accuracy and time saving



UCLA Health

Automated segmentation methods

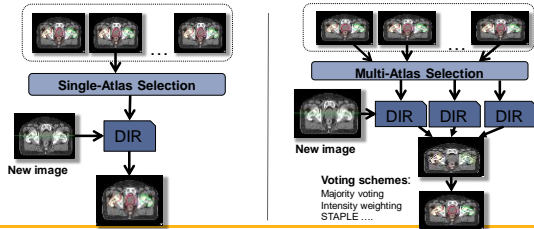
- Non prior-knowledge
 - Directly based on image voxel intensities and/or gradient
 - High contrast structures e.g. lung, bone, air cavity
- Prior-knowledge
 - Atlas based segmentation
 - Statistical model based segmentation: Shape (SSM) or Appearance (SAM)
 - Machine learning based segmentation
 - Hybrid segmentation

Sharp et al. Medical Physics, Vol. 41, No. 5, 2014



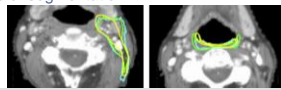
UCLA Health

Atlas based segmentation



Performance of atlas based segmentation

- Quality of atlas images and reference contours
- Atlas selection strategy: robust metric
- No consensus on database size
- Multiatlas can improve robustness of segmentation
 - Prone to topological error
 - Voting scheme is crucial
- Combination of Multimodality images (MRI and CT)



Single atlas - yellow Multiatlas - turquoise Reference -green
D. Teguh et al. Int. J. Rad Onc Biol. Phys., Vol. 81(4), 2011

Atlas based segmentation - DIR

- Quality of segmentation highly relies on deformable image registration (DIR)
- Ground-truth is not available
- Many different approaches and transformation modes

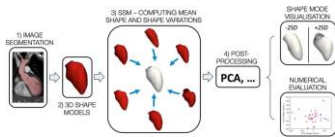
Table II. Commonly used transformation modes. (N = number of modes in an image)

Class	Transformation	Maximum dimensionality of transformation	Description
Geometric	Rigid	6	Allows translation in 3 dimensions and rotation about 3 axes
	Atlas	12	In addition to translation, allows uniform scaling and shear (e.g. parallel flow map parallel ¹⁰⁷)
	Free form	2N	Local, voxel-based deformation, often regularized by a smoothing parameter
	Global affine based methods (e.g., B-spline splines)	2N	Parametric deformable using a sparse grid of basis function control points with associated global influence (e.g., deformation is global ¹⁰⁸)
	Local affine based methods (e.g., B-splines)	2N	Parametric deformation using a weighted grid of control points of basis functions with local influence (e.g., deformation is local ¹⁰⁹)
Physical	Viscoelastic/plastic flow (e.g., demons)	2N	Nonlinear viscoelastic displacement field displacement by a vector field is a diverging gradient. In iterative gradient descent method is local ¹¹⁰
	Phase domain methods (PDM)	2N	Sparsely sampled non-displacement voxel displacements, generated by biomechanical linear properties (displacement is local ¹¹¹)

Brock et al. Med. Phys. 44 (7), July 2017

Statistical model based segmentation

- Confine the segmented contours to anatomically plausible shape or appearance
- Require training dataset to characterize variation of shape or appearance of structure
- Fit the test image to the model based on image intensities, gradients, features etc.

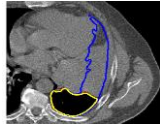


Biglino et al. Heart, 2016 0:1-6



Machine-learning based segmentation

- Outstanding performance in classification, detection, pattern recognition
- Automatically learn priors for structures or image context and tissue appearance
- Require training and significant computational resource
- Usually combined with shape model or atlas based methods



Lustberg et al. Radio and Onc 126 (2018)



11

Segmentation for adaptive planning

- Intra-object segmentation for anatomy at two different time points
- Deformable image registration is the most popular method
- Time constraints require very robust and accurate segmentation



Lamb J, Cao M, Kishan A, et al. Cureus 9(8): e1618





Methodological Review

A review of segmentation and deformable registration methods applied to adaptive cervical cancer radiation therapy treatment planning

Sumanya Ghose^{a,*}, Loni Holloway^{a,b,c,d}, Karen Lim^a, Philip Chan^a, Jacqueline Vieira^a, Shuhua Bi, Vinod^{a,b}, Gary Linzy^a, Peter B. Green^a, Jason Dowling^a



- Literature review of segmentation and registration methods for adaptive cervical cancer treatment planning:
 - Landmark, rigid, B-spline, shape constrained B-spline registration
- A average of 0.85 Dice similarity and mean surface distance of 2-4mm
- The use of **shape priors** significantly improved segmentation accuracy



Evaluation of segmentation performance

- | | |
|---|---|
| <ul style="list-style-type: none"> • Geometric <ul style="list-style-type: none"> • Moment based <ul style="list-style-type: none"> • Center/Volume of structure • Overlap based <ul style="list-style-type: none"> • Dice similarity coefficient • Distance based <ul style="list-style-type: none"> • Average/maximum distance • Intra-observer variability | <ul style="list-style-type: none"> • Dosimetric <ul style="list-style-type: none"> • Dose optimization • Dosimetric metrics (DVHs) • Clinical decision |
|---|---|

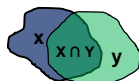
Sharp et al. Medical Physics, Vol. 41, No. 5, 2014



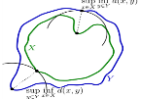
Geometry based evaluation

- Dice similarity index (DSI)
 - Insensitive to large structure
 - insensitive to fine details
- Hausdorff distance (HD)
 - Sensitive to small regions
 - Usually use 95% percentile
- May not correlate with each other
- Do not relate to dosimetry!

$$D = \frac{2|X \cap Y|}{|X| + |Y|}$$



$$d_H(X, Y) = \max \left\{ \sup_{x \in X} \inf_{y \in Y} d(x, y), \sup_{y \in Y} \inf_{x \in X} d(x, y) \right\}$$



Inter-observer variability

- A single manual contour may not truly represent the ground truth
- Inter-observer and Intra-observer contour variations exist
- Consensus on contour definition is not always available
- Inter-observer variability should be used as benchmark to assess the accuracy and robustness of auto-segmentation



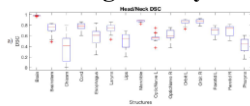
Medical Physics

Table 1. Inter-observer variability and automatic segmentation accuracy of selected organs.

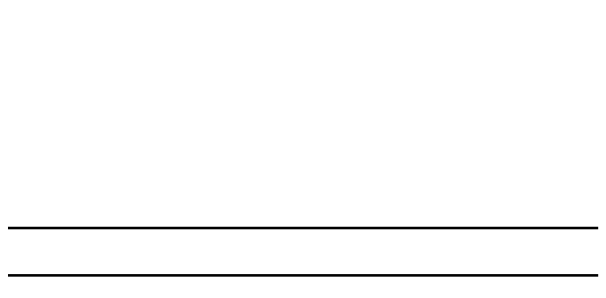
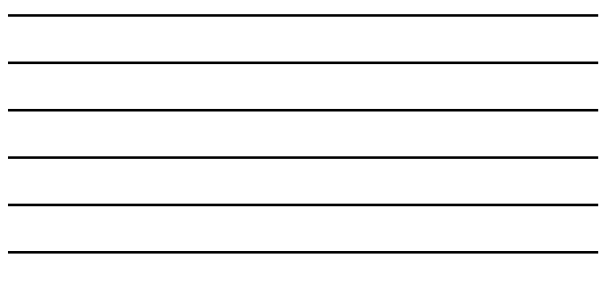
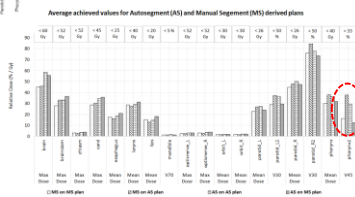
Site	Evaluation	Inter-observer variability	Automatic segmentation accuracy
Head	Contour	0.91 ± 0.04 (Ref. 45)	0.72 (Ref. 46)
	Brain	0.91 (Ref. 45)	0.86 (Ref. 47)
	Brain	0.98 ± 0.01 (Ref. 48)	0.83 (Ref. 46)
	Brain	0.97 ± 0.01 (Ref. 49)	0.86 (Ref. 50)
Breast	Contour	0.93 ± 0.01 (Ref. 51)	0.88 ± 0.01 (Ref. 52)
	Contour	0.93 ± 0.01 (Ref. 51)	0.88 ± 0.01 (Ref. 52)
	Contour	0.94 ± 0.01 (Ref. 53)	0.77 (Ref. 46)
	Contour	0.94 ± 0.01 (Ref. 53)	0.84 (Ref. 54)
Lung	Contour	0.81 ± 0.11 (Ref. 55)	0.72 (Ref. 56)
	Contour	0.87 ± 0.08 (Ref. 56)	0.61 (Ref. 56)
	Contour	0.87 ± 0.08 (Ref. 56)	0.44 (Ref. 56)
	Contour	0.87 ± 0.08 (Ref. 56)	0.52 (Ref. 56)
Parotid gland	Dice	0.85 (Ref. 59)	0.85 ± 0.03 (Ref. 61)
	Jaccard	0.66 ± 0.11 (Ref. 52)	0.73 (Ref. 59)
	CT	0.76 ± 0.08 (Ref. 49)	0.74 (Ref. 50)
	CT	0.43 (Ref. 56) (Ref. 57)	
		0.60 (Ref. 53)	
		0.26 (Ref. 73) (Ref. 60)	
Rectal (small intestine)	Contour	0.76 ± 0.17 (Ref. 58)	0.72 (Ref. 56)
	Contour	0.85 (Ref. 58)	0.60 (Ref. 56)
	Contour	0.98 ± 0.01 (Ref. 52)	0.81 ± 0.01 (Ref. 62)
	Contour	0.93 ± 0.01 (Ref. 48)	0.73 (Ref. 46)
Pancreas	Contour	0.81 (Ref. 57)	0.76 (Ref. 56)
	Contour	0.81 (Ref. 57)	0.76 (Ref. 56)
	Contour	0.81 (Ref. 57)	0.76 (Ref. 56)
	Contour	0.81 (Ref. 57)	0.76 (Ref. 56)



From geometry to dosimetry



Stiehl B et al. AAPM 2017



Mandible:

- Exclusion of teeth
- Image artifacts from dental implant

AAM - active appearance model
SSM - statistical shape model



Team	IM	FH	UW
Method	AAM	SSM	Image Processing
Dice	0.93	0.785	0.728
95%HD(mm)	2.041	5.919	29.458



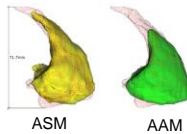
Raudaschl et al.: Medical Physics, 44 (5), 2017



Parotid glands:

- Large shape variation
- Poor soft tissue contrast
- Heterogeneous tissue including vessels and ducts

Team	Dice	Max HD (mm)
UB	0.814	12.000
IM	0.826	30.490



Raudaschl et al.: Medical Physics, 44 (5), 2017



More on segmentation challenge

- AAPM 2017 Thoracic Auto-segmentation Challenge
- RTOG 1106 contouring atlas
- 36 training sets, 12 offsite test and 12 live competition cases
- Intra-observer contour variability considered

• Xiao Han (Elekta Inc.)
Automatic Thoracic CT Image Segmentation using Deep Convolutional Neural Networks

• Xue Feng (University of Virginia)
A 3D UNet based thoracic segmentation framework using cropped images

• Bruno Oliveira (University of Minho)
Automatic Multi-organ Segmentation in 3D Computed Tomography



<http://autocontouringchallenge.org>



Summary

- Automated segmentation has shown promising performance in contouring for treatment planning
- Improvement on robustness, accuracy and throughput is still needed:
 - Consensus on contouring and benchmark database
 - Standardization of imaging acquisition; improvement of image quality; combination of multiple image modalities
 - Advancement in model and machine-learning based algorithms
 - Quality metrics and QA tools for spatial and dosimetric uncertainties
 - Effective translation from research to clinic with sufficient user training



UCLA Health

Acknowledgement

- Dr. Dan Ruan
- Dr. Ke Sheng
- Brad Stiehl



UCLA Health
